Estimation of Fire-induced CO Plume Age from NAST-I During the FIREX-AQ Field Campaign

Daniel K. Zhou,* Allen M. Larar, Xu Liu, and Xiaozhen Xiong
NASA Langley Research Center, Hampton, VA 23681, US

Abstract. Ultra-spectrally resolved infrared measurements from aircraft and space-based observations contain information about tropospheric carbon monoxide (CO) and ozone (O_3), as well as other trace species. A methodology for retrieving these tropospheric trace species from such remotely sensed spectral data has been developed and validated for the National Airborne Sounder Testbed-Interferometer (NAST-I). The Fire Influence on Regional to Global Environments and Air Quality (FIREX-AQ) field campaign was conducted during August 2019 to investigate the impact of wildfire and biomass smoke on air quality and weather in the continental United States. NAST-I CO and O_3 measurements from the recent FIREX-AQ field campaign are presented herein and used to estimate wildfire plume age. Results show enhanced levels of CO in the evolving plume as it is transported away from the fire ground site, and its plume age associated with the plume distance in both vertical and horizontal directions from the wildfire location. These results are enabled by the moderate-vertical and high-horizontal resolution obtained from the NAST-I IR spectrometer onboard NASA ER-2 aircraft. This study advances our knowledge of fire-induced plumes with their evolution and age characterized in 3-dimensional space using information from NAST-I retrieved CO and O_3 and relative changes in their concentrations.

Keywords: Plume age, ozone, carbon monoxide, wildfires, infrared measurements, remote sensing.

*Daniel K. Zhou, E-mail: daniel.k.zhou@nasa.gov

1 Introduction

In recent decades, wildfires have gained more of our attention as their number of occurrences, sizes, and intensities have significantly increased, likely due to climate change, or dryer and hotter conditions. Wildfire-induced pollutants and smoke (i.e., poor air quality) pose great risks to human health although wildfires can be an important natural event in many ecosystems. Chemistry and composition of smoke from wildfires are being studied to improve our understanding of the relationship between combustion and air quality, weather, and climate and the ability to forecast.[1]

Carbon monoxide (CO) is one of the major pollutants due to combustion.[2] The significance of CO in atmospheric chemistry was recognized long ago when a photo-chemically driven chain reaction was recognized linking the tropospheric cycles of CO, methane (CH_4), and ozone (O_3)

with those of the hydroxyl radical (OH) and hydroperoxyl radical (HO_2).[3] O_3 as another major pollutant can also cause several health problems to human beings.[4] O_3 plays a significant role in tropospheric chemistry; and details on ozone production from wildfires can be found from other studies.[5,6] Previous studies and observations suggested some degree of O_3 production as wildfires generate emissions of O_3 precursors, such as NO_x ($NO+NO_2$) emitted from wildfires thus increasing PAN (peroxyacetyl nitrate) as well.[6] O_3 production decreases quickly downwind of combustion.[7] However, O_3 production can be complicated and depend upon many factors, e.g., aerosols in a biomass plume from a wildfire reduce the photolysis rates of NO_2 and O_3. The impact of lower photolysis rates on O_3 production is not clear. Reducing the photolysis rates can either increase or decrease the net O_3 production by changing both the O_3 production and loss rates.[6] O_3 plume characteristics from wildfires are not as obvious as that for CO plumes because O_3 is not directly produced by wildfires, and it has a short lifetime in comparison to that of CO. However, both CO and O_3 within wildfire plumes are particularly interesting as they are related to the plume age and associated plume evolution and transport. Observations were made of $\Delta O_3/\Delta CO$ due to wildfires for biome and plume age,[6] indicating a positive relationship between $\Delta O_3/\Delta CO$ and plume age. Tropospheric chemical reactions involving CO extend their influence on air quality and global climate through accumulation of greenhouse gases. CO can be transported a great distance from its original source due to its relatively long lifetime (averaging about 2 months) in the troposphere.

The Fire Influence on Regional to Global Environments and Air Quality (FIREX-AQ) experiment, during August 2019 is the first joint field campaign conducted by NOAA and NASA addressing wildfire emissions and their impact on air quality and climate. It was dedicated to the sampling and characterization of fires and their impact on air quality and weather from the point

of trace species emissions.[8,9] Ground, airborne, and satellite measurements were made during the FIREX-AQ field phase. The National Airborne Sounder Testbed-Interferometer (NAST-I) is an airborne interferometer sounding system. It provides a highly spatial linear resolution that is equal to 13% of the aircraft altitude at nadir and 13 instrument field-of views (IFOVs) across the aircraft track from 13 scan angles (i.e., 2.6 km IFOV, ~3.4 km apart on the ground from ER-2 altitude of 20 km). NAST-I spatially scans and provides high-spectral resolution (0.25 cm^{-1}) measurements within the spectral region of 645–2700 cm^{-1}.[10-15] Here we use measurements from NAST-I on board the NASA ER-2 aircraft to study fire-induced CO plumes. NAST-I continuously covers a space large enough to monitor the wildfire plume from its origination, evolution and transport, providing 3-dimenstional (3-d) distributions of geophysical parameters including O_3 and CO with a higher spatial resolution comparing to satellite IR-ultraspectral sensors and thus, benefits our study of wildfire plumes.[16] NAST-I data used in this ~~letter~~ study were collected under clear-sky conditions. Geophysical parameters cannot be retrieved with NAST-I under opaque clouds as infrared measurements are not able to penetrate opaque clouds.[14] Materials presented in this ~~letter~~ study are a follow-up to the work of Zhou et al.[16] A brief description of the FIREX-AQ experiment, observations, and wildfire plume age estimation methodology will be given in Section 2. Results and discussion are presented in Section 3. Summary and concluding remarks follow in Section 4.

2 Experiment, Observation, and Plume Age Estimation Methodology

FIREX-AQ is a multi-disciplinary effort campaign with multi-agency collaborations to study complex fire systems. Research platforms were heavily instrumented with in-situ and remote-sensing devices to allow exhaustive characterization of gases and aerosols, optical properties, wind fields, fire radiative power and more. Ground-based examinations of fuels and burned areas

81 permitted clearer connections between atmospheric pollutants and their sources. Modeling efforts
82 were used during the campaign to predict transport, and study emissions and downwind plume
83 transformations.

84 The results presented here are based upon CO and O_3 retrievals from NAST-I measurements.
85 The NAST-I instrument, and its retrieval algorithms are described elsewhere.[10-19] The western
86 portion of the FIREX-AQ campaign domain (August 5–21, 2019) covers 14 large wildfires fueled
87 by grass, woodland, and scrub.[20] Fire-induced CO plumes observed by NAST-I during the
88 FIREX-AQ have been analyzed and reported.[16] For this study of wildfire plume age, we have
89 chosen the ER-2 sorties over the William Flats fire and the extended downwind area from August
90 7, 2019, as the ER-2 sorties have ~450 km downwind flight leg segments. The William Flats fire
91 was caused by lightning on August 2, 2019. It covered approximately 100 km^2 and was located at
92 about 11 km southeast of Keller, Washington. The ER-2 flew from west (-120º longitude) to east
93 (-113º longitude), then back west at a near-constant latitude, passing over the fire location (48.0º
94 latitude, -118.5º longitude) and the extended downwind area to detect fire-induced gas emissions
95 and characterize their subsequent evolution. A large downwind area covered by the ER-2 flight
96 makes an excellent naturally occurring experiment to study fresh and aged plumes.

97 Geophysical parameters such as temperature, moisture, CO and O_3 profiles are retrieved from
98 NAST-I measured spectral radiances. The NAST-I retrieval algorithm was developed, tested,
99 improved, and validated.[13,14,17] The NAST-I trace gas (CO and O_3) retrieval algorithm was also
100 developed[18] and later improved by implementation of a surface emissivity retrieval.[19] During the
101 FIREX-AQ field campaign, CO retrievals are validated by using in-situ measurements from the
102 NASA DC-8 aircraft.[16] There are two O_3 in-situ sensors flying on the DC-8 aircraft: one is the
103 NOAA Nitrogen Oxides and Ozone (NO_yO_3) 4-channel chemiluminescence instrument[21] and the

other is the Rapid Ozone Experiment (ROZE).[22] The nature of O_3 (e.g., its lifetime and photochemical reactions) and its impact on the atmosphere from wildfires is not as obvious as that of CO. O_3 is relatively stable in comparison with fire-induced CO, which makes it a bit easier for inter-comparison between NAST-I remotely sensed and in-situ measured ozone. A few DC-8 sorties were spatially coincident with the ER-2 sorties at the same fire locations but, in general, they had lag times of a few hours. There was one exception wherein both spatial and temporal coincidence was achieved between the two aircraft, specifically, on August 6, 2019.[16] Here we use the 60-second merged data from DC-8 measurements available from the FIREX-AQ database[23] to ~~inter~~compare with NAST-I O_3 retrievals. Inter-comparison between ER-2 NAST-I O_3 and DC-8 in-situ O_3 are made in the vicinity of the William Flats fire location from data collected on August 6–8, 2019. Fig. 1a plots the NAST-I O_3 (in black open circles) and in-situ O_3 data (the mean of ROZE and NO_yO_3 measurements, in black asterisks) with a coincidence spatial-criteria of $|\Delta(\text{latitude})| < 0.05^o$ and $|\Delta(\text{longitude})| < 0.05^o$ and temporal-criteria of $|\Delta(\text{UTC})| < 1.0$ hr. for August 6, 2019. The NAST-I O_3 profile is interpolated to DC-8 in-situ altitude. Fig. 1b shows the difference between NAST-I and in-situ O_3 plotted in Fig. 1a. Similar data from August 7 and 8, 2019, are also plotted (in red and blue symbols, respectively) with a relatively larger temporal-criteria of $|\Delta\text{UTC}|$ as shown in Fig. 1c. Overall, from the data shown in Fig. 1, the mean error (bias) and standard deviation error (STDE) between NAST-I retrievals and in-situ measurements are 7.55 (ppbv) and 10.85 (ppbv), respectively. Reasonable agreement between the ER-2 NAST-I and DC-8 in-situ O_3 measurements is achieved with some differences due to their spatial and temporal mismatches. However, it is noticed that NAST-I O_3 starts to deviate from in-situ measurements at an altitude of <= 3 km. This is believed to be a consequence of the expected lower ozone retrieval sensitivity in the NAST-I passive infrared measurements at an altitude region

below 3 km ~~caused by a large amount of O_3 from higher altitudes in the lower stratosphere~~. However, the uncertainty of ΔO_3 is relatively small compared to that of O_3 itself as the retrieval uncertainties of the polluted and clean background O_3 regions are similar. From this evaluation, we believe that NAST-I O_3 retrievals are reasonably good at the altitude of 3 km and above and can be used together with CO retrievals to estimate the age of wildfire-induced plumes as presented in the following section.

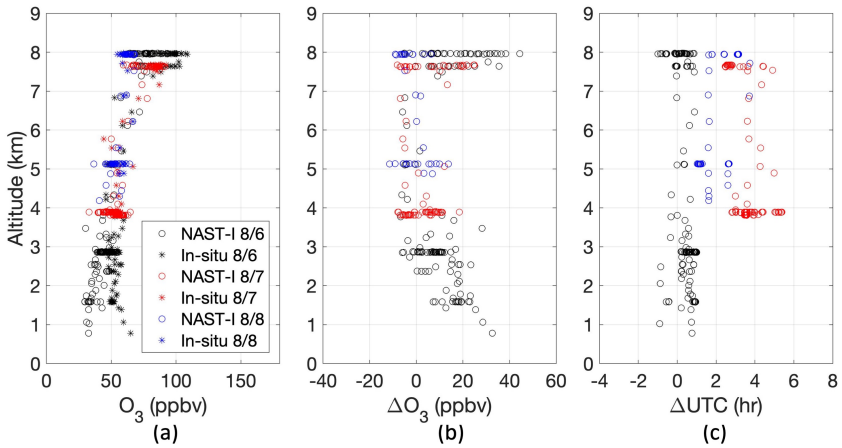

Fig. 1 NAST-I O_3 retrieval evaluation with in-situ measurements near William Flats fire location from August 6–8, 2019, in black, red, and blue, respectively (see text). (a) NAST-I retrieved and In-situ measured O_3, (b) the difference between NAST-I and In-situ O_3, and (c) the UTC difference between NAST-I and In-situ O_3 measurement.

The William Flats fire progression and CO plume evolution during August 6–8 2019 were observed by multiple airborne sensors including NAST-I.[16] NAST-I CO retrieval uncertainty has been evaluated with the co-incident In-situ measurements, and found to have a bias of ~8 ppbv and standard deviation of difference (STDE) of ~28 ppbv.[16] The NAST-I measurements provide 3-d distribution of temperature, water vapor, CO, and O_3. For the case study here, the ER-2 sorties went over the William Flats fire and the extended downwind area twice. NAST-I retrieved cross sections in nadir view are plotted in Fig. 2 for one sortie (from west to east); the retrievals from the return sortie are almost identical. Moisture layers are shown in relative humidity (RH) with

147 less saturation (<100%) indicating clear-sky conditions in the observations. CO plumes in the
148 downwind area are evidently clear. The O_3, plotted in a logarithmic scale, illustrates its small
149 variation in free troposphere from the ground level up and its enhancement over the fire location
150 (-118.5º longitude).

151 Fire-induced plumes contain information on chemical gaseous photochemical reaction and
152 production; it is essential to know the plume's evolution and age to better understand impacts to
153 air quality, weather, and climate. Fire plume age has been widely measured and studied by
154 numerous researchers. Observations of $\Delta O_3/\Delta CO$ due to wildfires by biome and plume age were
155 summarized by Jaffe and Wigder.[6] Many factors contribute to O_3 production within wildfire
156 plumes. In general, Jaffe and Wigder found a positive relationship between the $\Delta O_3/\Delta CO$ ratio
157 and plume age. Here we assume this relationship is a linear $T = \alpha R + \beta$, where T is plume age in
158 hours and R is $\Delta O_3/\Delta CO$ ratio. α and β are the slope and intercept, respectively. A fitting
159 relationship is obtained from Table 1 of Jaffe and Wigder.[6] For boreal and temperate regions
160 (BTR), α=327.2 and β=89.4; while for the tropical and subtropical regions (TSR), α=215.8 and
161 β=3.1. The $\Delta O_3/\Delta CO$ ratio increases as the plume ages, and it ages relatively slower in tropical
162 and equatorial regions as more O_3 production expected from more NO_x emissions per unit of fuel
163 consumed.[6] Based upon this assessment, our plume age estimation methodology relies on
164 $\Delta O_3/\Delta CO$ ratios within the plumes.

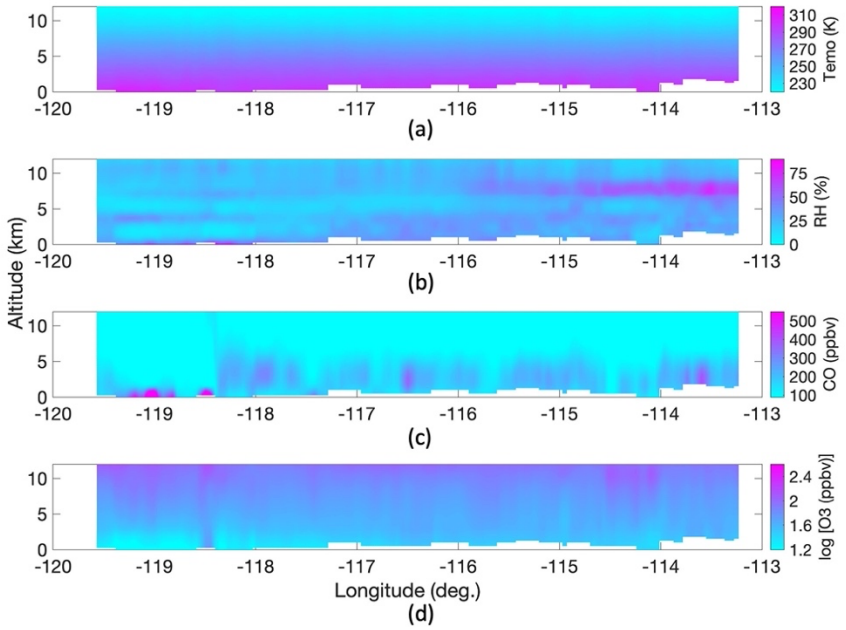

Fig. 2 NAST-I retrieval cross sections in nadir view for (a) temperature (K), (b) relative humidity (%), (c) CO (ppbv), and (d) O_3 (ppbv) in logarithmic scale.

Within fire-induced CO plumes, we assume that CO concentrations are greater than 135 ppbv. Subtracting the background estimates, ΔO_3 and ΔCO are calculated using NAST-I retrieved O_3 and CO. O_3 background is assumed to be the average of its regional climatology which is from a global climatology database that consists of 15,150 profiles obtained from the extended SeeBor database of Univ of Wisconsin-Madison[23,24] and NAST-I retrieval mean, while CO background is assumed to be its regional climatology. 3-d distributions of ΔO_3 and ΔCO within the plumes (where CO > 135 ppbv) are plotted in Figs. 3a and 3b, respectively, along the longitude with a color distribution in altitude. It is noted that elevated O_3 spans at least 26 km near the fire location (-118.5º longitude) and covers an area of 531 km^2. It is worth mentioning that ΔO_3 and ΔCO plotted in Fig. 3 are estimations as O_3 and CO background within the plumes are not precisely known but made to the best of our knowledge and assumed to be the same throughout the local region.

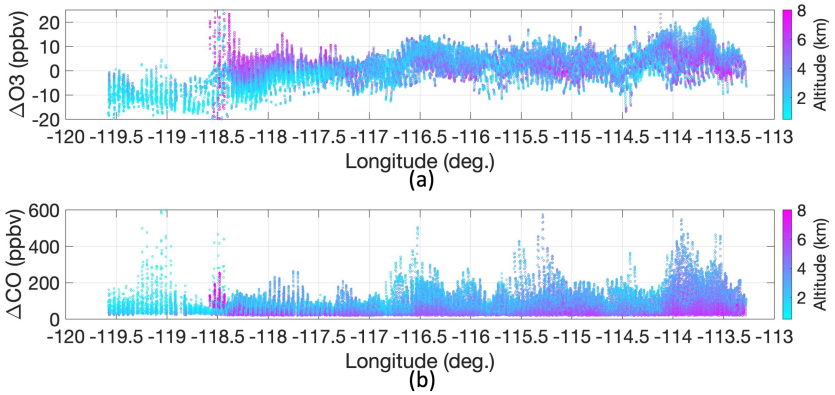

Fig. 3 (a) ΔO_3 and (b) ΔCO distribution within the fire-induced plumes.

3 Results and Discussion

The $\Delta O_3/\Delta CO$ ratio is estimated from retrievals using NAST-I flight observations and plotted in Fig. 4a. CO plume age can be simply projected from wildfire $\Delta O_3/\Delta CO$. For the William Flats fire location (48.0º latitude), a linear combination of 55% BTR and 45% TSR coefficients are used to calculate the plume age that would reflect a near fresh plume at the fire location. Estimated plume age is plotted in Fig. 4b. For plumes at a lower altitude (i.e., 4 km and below), their ages increased as the plumes moved away from the fire location downwind and merged with aged plumes (~60–100 hr.) while other aged plumes were sitting at a higher altitude (4 km and above).

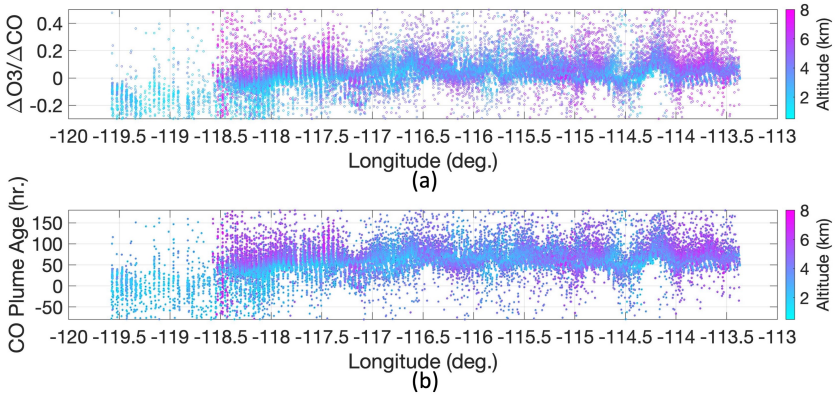

Fig. 4 (a) $\Delta O_3/\Delta CO$ distribution along the longitude within the fire-induced plumes, and (b) estimated plume age distribution.

Fig. 5a plots the plume age along the longitude with error bars indicating its variation over

197 altitude and longitude. Fresh plumes were observed to be closer to the fire location while aged
198 plumes were in the downwind regions as expected. Figs. 5b-5c plots the mean plume age against
199 the altitude with an error bar indicating its variation over longitude and latitude. The ages depend
200 on the distance (e.g., longitude) from the fire location. Fig. 5b covers all data shown in Fig. 5a;
201 Figs. 5c and 5d have data plotted where longitude is less than and greater than -117º, respectively.
202 Near the fire location, shown in Fig. 5c, fresh plumes are at a lower altitude and plume ages
203 increase as altitude increases. As the plumes move further downwind, as shown in Fig. 5d, fresh
204 and aged plumes were mixed along the altitudes with a near constant mean plume age of ~50 hours,
205 but with a large variation (i.e., a large standard deviation) indicated by the error bars (reduced by
206 a factor of 5 for clarity) in the altitude region of ~3.5–7.0 km, where a greater mixture of fresh and
207 aged plumes co-exist. In general, as shown in Fig. 4b, fresh plumes were at a lower altitude while
208 aged plumes were found in the upper regions. Lastly, the distributions of enhanced CO column
209 density from the fire plume and the vertical mean CO plume age (VMCOPA) are plotted in Figs.
210 6a and 6b, respectively. It is worth noting that there are two flight tracks (2 legs) back and forth
211 with time evolution on top of each other, only the first leg is plotted in Fig. 6 for clarity. Comparing
212 CO column density and its vertical mean CO plume age, a large amount of relatively fresh CO
213 plumes was near the fire location and aged CO plumes had been transported further downwind
214 and/or upper regions.

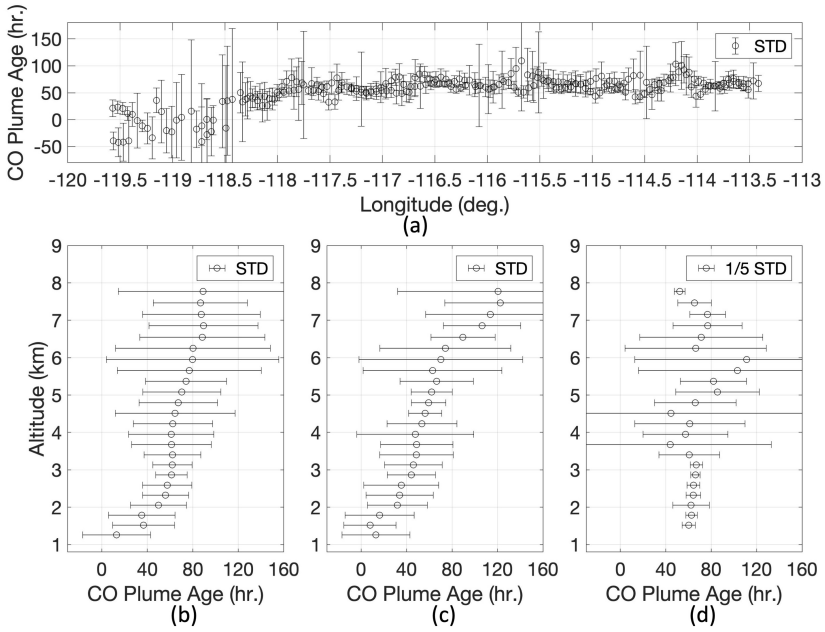

Fig. 5 (a) Plume age distribution along the longitude. Plume age distribution along the altitude: (b) all data shown from (a), (c) data from longitude less than -117.0º (near fire location), and (d) data from longitude greater than -117.0º (further away from fire location).

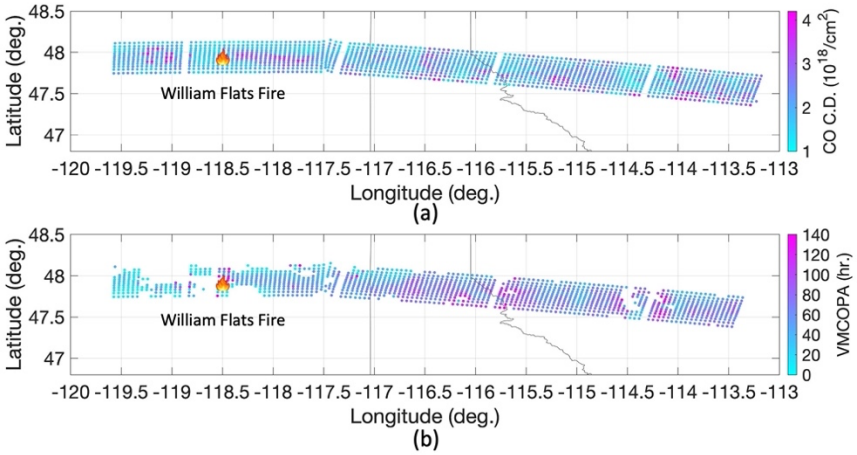

Fig. 6 Distribution of (a) CO column density and (b) vertical mean CO plume age (VMCOPA).

The William Flats fire started on August 2, 2019, and the oldest plumes could be 4–5 days old. The plume ages could be from mixed plumes (or effective plumes) as indicated in Figs 4-6; therefore, in the area farthest away from the fire location, they could be somewhat less than 5 days old in our estimations. Nevertheless, the plume age distributions, both horizontally and vertically (shown in Figs. 5-6), make sense for the way plumes are transported and aged. The error or

uncertainty of plume age derived here is largely due to (1) O_3 and CO retrieval error especially at lower altitudes (3 km and below) as retrieval sensitivity decreased, (2) the uncertainty from estimated CO and O_3 background within the plume, (3) the limited data available for deriving the relationship between the plume age and ΔO_3 to ΔCO ratio, and a large data scattering and uncertainty in the dataset[6], (4) a linear fitting relationship between the plume age and $\Delta O_3/\Delta$CO ratio may not be the best representation, and (5) mixed (or effective) plumes being assessed, possibly contain contributions from multiple fire sources, especially in locations further away from the primary fire location.

Currently these error sources are not completely quantified, therefore, the plume age presented in this ~~letter~~ study is only an estimation. Regardless, however, it is critically important even though it may lack some quantitative accuracy since it nicely demonstrates the ability to characterize wildfire plumes and estimate their age from the perspective of an advanced ultraspectral infrared remote sounder. CO and O_3 retrievals are the mean over the IFOV with a vertical column resolution. The plume we dealt with is an effective plume or a volume mean of mixed plumes. The plume age presented herein is also an effective mean plume age in the NAST-I sensor IFOV, which can be different from in-situ measurements.

It is worth mentioning that the North Hills fire, started on July 26, 2019, was located at about 5 km northwest of Lake Helena, Montana (46.8º latitude, -112.0º longitude). It covered approximately 20 km^2. CO plumes from the North Hills fire are unlikely but could contribute to the data presented here at the locations near the western (possibly upwind) areas of the North Hills fire location.

4 Summary and Concluding Remarks

The FIREX-AQ field campaign with multiple aircraft in-situ and remotely sensed observations

provides characterization of distributions of chemical species induced by wildfire emissions and subsequent evolution. This unique dataset is very much desirable in validating NAST-I O_3 and CO retrievals and illustrates the benefits of such data for wildfire characterization. The Wildfire case of Williams Flats from the FIREX-AQ experiment reported herein is used to demonstrate a fire-induced plume age estimation approach. Several major summary items and conclusions can be obtained from this work. (1) NAST-I remotely sensed O_3 is evaluated by favorable inter-comparisons with the in-situ O_3 measurements which show a positive agreement (shown in Fig. 1). (2) Small but significant enhanced O_3 production near William Flats wildfire location is observed by NAST-I. (3) O_3 and CO productions impacted by the wildfire are estimated within the fire-induced plume. (4) Plume age is estimated using NAST-I observed $\Delta O_3/\Delta CO$ ratios and a linear fitting relationship from previous observations of wildfire $\Delta O_3/\Delta CO$ ratios by biome and plume age.[6] (5) Plume age distribution both horizontally and vertically indicates how the plume ages as it moves away from the fire location (for William Flats Fire case).

It was reported earlier that first-of-a-kind wildfire-induced plume measurements were obtained by the NAST-I ultraspectral remote sensor on board the ER-2 suborbital aircraft, which has shown the intensity and size of wildfire plumes in a high-spatial-resolution of 2.6 km. Now, in the present study, the plume age estimation in a 3-d high-spatial-resolution adds critical temporal information of the fire-induced plume, demonstrating the capability of an ultraspectral remote sensor like NAST-I with a higher spectral and spatial resolution to monitor CO and O_3 and its advantage of giving broader spatial and temporal assessment by rapidly covering a large field of observation. This work demonstrates 3-d plume age estimation and advances our measurement ability to observe fire-induced plumes and characterize their evolution and age.

NAST-I was successfully operated during all ER-2 flights of the FIREX-AQ experiment (a

total of 11 flights and 50+ hours of science data collected). NAST-I retrievals (e.g., atmospheric temperature, relative humidity, CO, and O_3 profiles, also surface skin temperature), together with experiment data from other satellite/aircraft/ground measurements and analysis from the FIREX-AQ campaign are available[253] for the science community to study wildfire-related topics as described by the overarching objective of FIREX-AQ experiment[8] and beyond.

Acknowledgments

The authors greatly appreciate the FIREX-AQ management team, aircraft pilots and crew of NASA ER-2 and DC-8. O_3 in-situ data were provided by ROZE team (Principal Investigators Drs. R. A. Hannun and T. F. Hanisco) and NOAA NO_yO_3 team (Principal Investigator Dr. T. B. Ryerson). The authors wish to thank A. M. Noe of NASA Langley Research Center and L. Rochette of LR Tech, Inc. for their dedicated support of NAST-I instrument upgrade, maintenance, and field mission. The authors wish to acknowledge Dr. J. A. Kaye of the NASA Science Mission Directorate and Dr. M. D. Goldberg of NOAA NESDIS for their continued, enabling support of the NAST-I program. The authors wish to thank one anonymous referee for his/her useful comments and suggestions. The NAST-I is part of the Airborne Science Program within the NASA Earth Science Division.

References

1. P. J. Crutzen, L. E. Heidt, J. P. Krasnec, W. H. Hollock, and W. Seiler, "Biomass burning as a source of atmospheric gases CO, H_2, N_2O, NO, CH_3Cl, and COS," *Nature*, **282**, 253–256 (1979).

2. J. Fishman, K. Fakharuzzaman, B. Cros, and D. Nganga, "Identification of widespread pollution in the Southern Hemisphere deduced from satellite analyses", *Science*, **252**, 1,693–1,696 (1991).

3. H. Levy, II, "Natural atmosphere: large radical and formaldehyde concentrations predicted," *Science*, **173**, 141–143 (1971).

4. J. J. Zhang, Y. Wei, and Z. Fang, "Ozone pollution: A major health hazard worldwide," *Frontiers in Immunology*, **10**, 2518 (2019).

5. H. B. Singh et al., "Pollution influences on atmospheric composition and chemistry at high northern latitudes: boreal and California forest fire emissions," *Atmospheric Environment*, **44**, 4,553–4,564 (2010).

6. D. A. Jaffe and N. L. Wigder, "Ozone production from wildfires: A critical review," *Atmospheric Environment*, **51**, 1-10 (2012).

7. E. V. Fischer, D. A. Jaffe, D. R. Reidmiller, and L. Jaegle, "Meteorological controls on observed peroxyacetyl nitrate at Mount Bachelor during the spring of 2008," *J. Geophys. Res*., **115**, D03302 (2010).

8. FIREX-AQ: Investigating smoke from wildfire and biomass burring. Accessed: Nov. 5, 2021. [Online]. Available: https://www.esrl.noaa.gov/csl/projects/firex-aq/.

9. D. A. Jaffe *et al.*, "Wildfire and prescribed burning impacts on air quality in the United States," *Journal of the Air & Waste Management Association*, **70**, 583–615 (2020).

10. The National Airborne Sounder Testbed-Interferometer (NAST-I), Accessed: Nov. 5, 2021. [Online]. Available https://airbornescience.nasa.gov/instrument/NAST-I.

11. D. Cousins and W. L. Smith, "National Polar-Orbiting Operational Environmental Satellite System (NPOESS) Airborne Sounder Testbed-Interferometer (NAST-I)," in *Application of*

Lidar to Current Atmospheric Topics II, A. J. Sadlacek III and K. W. Fischer, eds., *Proc. SPIE*, **3127**, 323–331 (1997).

12. W. L. Smith *et al.*, "NAST-I: results from revolutionary aircraft sounding spectrometer," in *Optical Spectroscopic Techniques and Instrumentation for Atmospheric and Space Research III*, A. M. Larar, ed., *Proc. SPIE*, **3756**, 2–8 (1999).
13. D. K. Zhou, W. L. Smith, and A. M. Larar, "Tropospheric ozone near-nadir-viewing IR spectral sensitivity and ozone measurements from NAST-I," in *Hyperspectral Remote Sensing of the Land and Atmosphere,* W. L. Smith and Y. Yasuoka, eds., *Proc. SPIE*, **4151**, 277–284 (2001).
14. D. K. Zhou *et al.*, "Thermodynamic product retrieval methodology for NAST-I and validation," *Appl. Opt*., **41**, 6,957–6,967 (2002).
15. A. M. Larar *et al.*, "IASI spectral radiance validation inter-comparisons: case study assessment from the JAIVEx field campaign," *Atmos. Chem. Phys*., 10, 441–430 (2010).
16. D. K. Zhou et al., "Wildfire-induced CO plume observations from NAST-I during the FIREX-AQ field campaign," *IEEE J. Sel. Topics Appl. Earth Observ. Remote Sens.*, **14**, 2,901–2,910 (2021).
17. D. K. Zhou, W. L. Smith, Sr., X. Liu, A. M. Larar, S. A. Mango, and H.-L. Huang, "Physically retrieving cloud and thermodynamic parameters from ultraspectral IR measurements," *J. Atmos. Sci*., **64**, 969–982 (2007).
18. D. K. Zhou, W. L. Smith, X. Liu, J. Li, A. M. Larar, and S. A. Mango, "Tropospheric CO observed with the NAST-I: retrieval methodology, analyses, and first results," *Appl. Opt*., **44**, 3,032–3,044 (2005).

19. D. K. Zhou *et al.*, "Global land surface emissivity retrieved from satellite ultraspectral IR measurements," *IEEE Trans. Geosci. Remote Sens*., **49**, 1,277–1,290 (2011).
20. J. Schwarz and the FIREX-AQ Science Team, "The FIREX-AQ 2019 dataset is public," *EGU General Assembly 2020*, 4–8 May 2020, EGU2020-20755 (2020).
21. NOAA Nitrogen Oxides and Ozone ($NOyO_3$) instrument, Accessed: Nov. 5, 2021. [Online]. Available https://airbornescience.nasa.gov/instrument/NOyO3.
22. NASA Rapid OZone Experiment (ROZE), Accessed: Nov. 5, 2021. [Online]. Available https://airbornescience.nasa.gov/instrument/ROZE.
23. E. E. Borbas, S. W. Seemann, H.-L. Huang, J. Li, and W. P. Menzel, "Global profile training database for satellite regression retrievals with estimates of skin temperature and emissivity," Proc. Int. ATOVS Study Conf. XIV, Beijing, China, CIMSS, University of Wisconsin–Madison, 763–770, 2005.
24. S. W. Seemann, E. E. Borbas, R. O. Knuteson, G. R. Stephenson, and H.-L. Huang, "Development of a global infrared land surface emissivity database for application to clear-sky sounding retrievals from multi-spectral satellite radiance measurements," J. Appl. Meteorol. Clim., 47, 108-123, 2008.
25. NOAA/NASA FIREX-AQ campaign data archive. Accessed: Nov. 5, 2021. [Online]. Available: https://asdc.larc.nasa.gov/project/FIREX-AQ.

Caption List

Fig. 1 NAST-I O_3 retrieval evaluation with in-situ measurements near William Flats fire location from August 6–8, 2019, in black, red, and blue, respectively (see text). (a) NAST-I retrieved and

In-situ measured O_3, (b) the difference between NAST-I and In-situ O_3, and (c) the UTC difference between NAST-I and In-situ O_3 measurement.

Fig. 2 NAST-I retrieval cross sections in nadir view for (a) temperature (K), (b) relative humidity (%), (c) CO (ppbv), and (d) O_3 (ppbv) in logarithmic scale.

Fig. 3 (a) ΔO_3 and (b) ΔCO distribution within the fire-induced plumes.

Fig. 4 (a) $\Delta O_3/\Delta$CO distribution along the longitude within the fire-induced plumes, and (b) estimated plume age distribution.

Fig. 5 (a) Plume age distribution along the longitude. Plume age distribution along the altitude: (b) all data shown from (a), (c) data from longitude less than -117.0º (near fire location), and (d) data from longitude greater than -117.0º (further away from fire location).

Fig. 6 Distribution of (a) CO column density and (b) vertical mean CO plume age (VMCOPA).

Authors Biographies